

Masahisa Wada · Takeshi Okano · Junji Sugiyama

Allomorphs of native crystalline cellulose I evaluated by two equatorial d -spacings

Received: February 18, 2000 / Accepted: May 10, 2000

Abstract The aim of this study was to develop a facile method for categorizing native celluloses as the algal-bacterial type or the cotton-ramie type and for estimating the I_α/I_β (triclinic/monoclinic) ratio of the cellulose samples. We investigated various native celluloses by X-ray diffractometry; and discriminant analysis was carried out using two equatorial d -spacings: 0.59–0.62 nm (d_1) and 0.52–0.55 nm (d_2). All of the samples were classified into the two groups without error. The function used to discriminate between the two groups is represented as: $Z = 1693d_1 - 902d_2 - 549$, where $Z > 0$ indicates the algal-bacterial (I_α -rich) type and $Z < 0$ indicates the cotton-ramie (I_β -dominant) type. Another X-ray diffraction study of hydrothermally treated *Cladophora* cellulose revealed the relation between the d -spacings (d_1 , d_2) and the I_α/I_β ratio. A calibrating equation by which the I_α/I_β ratio was estimated from the two parameters, d_1 and d_2 , was then prepared. In the case of relatively highly crystalline native celluloses, it was found that the I_α/I_β ratio is easily determined by applying the two parameters in the equation.

Key words Hydrothermal treatment · X-ray diffractometry · Cellulose I_α · Cellulose I_β · I_α/I_β ratio

Introduction

There is general agreement that cellulose I is a composite of two crystalline modifications, I_α and I_β .^{1–4} Structures of cellulose I_α and I_β are assigned to the triclinic and monoclinic

systems, respectively.⁴ The latter, monoclinic form is thermodynamically stable because I_α can be transformed readily and entirely to I_β by hydrothermal treatment at 260°C.^{5–7} As first mentioned by Wada et al.,⁸ a relation between I_α/I_β dimorphism of cellulose and plant phylogenesis has been suggested owing to the I_α/I_β ratio varying as a function of plant species.⁹

The I_α/I_β ratio for cellulose from various origins has been investigated by many methods.^{8,10–13} Although the cellulose origins were roughly divided into I_α -rich type or I_β -dominant type, discussion about wood cellulose has continued.^{14–19} Using diffraction methods, the cellulose of wood and other higher plants was classified as the I_β -dominant type.^{14,15} By ¹³C nuclear magnetic resonance (NMR), however, the I_α/I_β ratio of wood cellulose was estimated to be 50:50.^{16–18} It has not been clearly elucidated why contradictory results with wood cellulose are obtained by different methods. A possible reason is that, with diffraction methods, I_α and I_β are interpreted to be crystals that form triclinic and monoclinic systems, respectively; and the results from ¹³C NMR may contain information about subcrystalline cellulose, which is a lower-ordered molecule than the crystals observed by the diffraction method. Particularly when investigating such lower crystalline cellulose as wood cellulose, therefore, we must recognize that the different methods probe somewhat different properties of the systems.

The aim of this study was to investigate systematically the structural variation among various cellulose origins. We tried to estimate the I_α/I_β ratio from the two equatorial d -spacings, which were measured using the standard X-ray diffraction method.

Materials and methods

Material

The vesicles of *Valonia ventricosa* and *Dictyosphaeria cavernosa* were harvested in the sea of Kuroshima, Okinawa. Whole plants of *Cladophora* sp. and

M. Wada (✉) · T. Okano
Department of Biomaterials Science, Graduate School of
Agricultural and Life Sciences, The University of Tokyo, 1-1-1
Yayoi, Bunkyo-ku, Tokyo 113-8657, Japan
Tel. +81-3-5841-5247; Fax +81-3-5684-0299
e-mail: wadam@sbp.fpa.u-tokyo.ac.jp

J. Sugiyama
Wood Research Institute, Kyoto University, Uji, Kyoto 611-0011,
Japan

Chaetomorpha crassa were collected in the seas of Chikura, Chiba and Suzuki, Shizuoka, respectively. A purified mat of bacterial cellulose was a gift from Rengo. The tunicates of *Halocynthia roretzi* were taken from a nursery in Kamaishi, Miyagi. A commercial cotton linter ACALA-SJ2 and bast fibers of ramie (*Boehmeria nivea*) and kouzo (*Braussonetia* sp.) were used. All samples were purified according to the method described in our previous papers.^{20,21} Briefly, samples were repeatedly treated in 5% KOH and 0.3% NaClO₂ aqueous solutions until they became perfectly white. After purification, they were disintegrated into small fragments with a double-cylinder type homogenizer.

In this study, we also used four kinds of wood powder: from akamatsu (*Pinus densiflora*), Douglas fir (*Pseudotsuga mensiesii*), yachidamo (*Fraxinus mandshurica*), and red meranti (*Shorea* sp.). The powders were purified by the same method as the other samples.

Hydrothermal treatment

Purified *Cladophora* was placed in a portable reactor with a small amount of 0.1N NaOH solution. The reactor was hermetically sealed and heated in a silicone oil bath to the required temperature between 200° and 280°C for 30 min. The reactor was then cooled in a large amount of water. The treated sample was taken out of the reactor and washed with deionized water by repeated centrifugation.

X-ray diffractometry

All samples were freeze-dried and reformed by pressing into disks at 200 kgf/cm² for 30 s. X-ray diffractometry in reflection mode was carried out on a RINT 2000 with monochromatic Cu-K_α radiation ($\lambda = 0.15418$ nm) using the following optical slit system: The divergence slit (DS) was 0.5°, the scattering slit (SS) was 0.5°, and the receiving slit (RS) was 0.15 mm. The scanning was performed as follows: The scattering angle (2θ) was 10°–30°; a step in 2θ of $\Delta 2\theta$ was 0.10° or 0.05°; and the time for each step (t) was 20 s.

Separation of peaks was carried out using the SALS²² program (Statistical Analysis with Least Squares Fitting), as described in our previous paper.¹² The fifth-degree polynomial function was used for a background of the profile, and the pseudo-Voigt (pV) function was used to represent each crystalline reflection. The pseudo-Voigt function $P(2\theta)_{pV}$ is

$$P(2\theta)_{pV} = \eta P(2\theta)_L + (1 - \eta)P(2\theta)_G \quad (1)$$

where η is an eta parameter varying from 0 to 1, and $P(2\theta)_G$ and $P(2\theta)_L$ are Gaussian and Lorentzian functions represented by the following equations:

$$P(2\theta)_G = \frac{2}{H} \left(\frac{\ln 2}{\pi} \right)^{1/2} \exp \left[-4 \ln 2 \left(\frac{2\theta - 2B}{H} \right)^2 \right] \quad (2)$$

$$P(2\theta)_L = \frac{2}{\pi H} \left[1 + 4 \left(\frac{2\theta - 2B}{H} \right)^2 \right]^{-1} \quad (3)$$

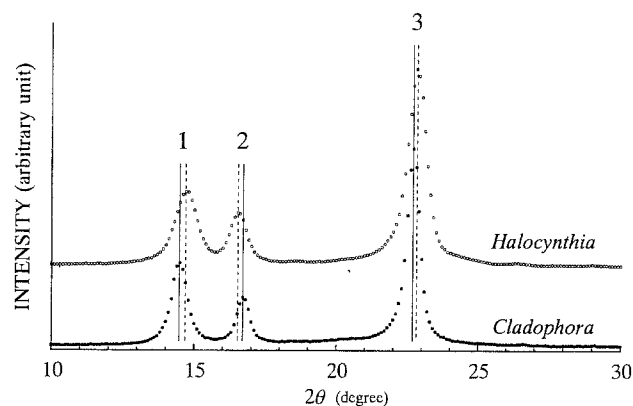


Fig. 1. X-ray diffractometry profiles of *Cladophora* and *Halocynthia* celluloses

where B is the Bragg angle, and H is the full-width at half-maximum (FWHM).

Results and discussion

Easy method to classify native celluloses into two types

We carried out X-ray diffractometry on various native cellulose samples. Figure 1 shows typical X-ray diffractometry profiles obtained from highly crystalline *Halocynthia* and *Cladophora* celluloses, which are I_β-rich and I_α-rich type celluloses, respectively. The three crystalline peaks in Fig. 1 appear in the 2θ range 10–30 degrees. The positions of these peaks are different for *Halocynthia* and *Cladophora* celluloses. This result is due to the varying I_α/I_β ratio in the samples because each peak is a composite of I_α and I_β reflections: peak 1 is I_α 100 and I_β 110; peak 2 is I_α 010 and I_β 110; and peak 3 is I_α 110 and I_β 200. When the I_β proportion in the sample increased, peaks 1, 2, and 3 shifted to higher, lower, and higher angles, respectively. To analyze these results further, we separated these three peaks and then calculated d -spacings and FWHM, which are listed in Table 1. All cellulose samples were classified as the algal-bacterial (I_α-rich) type or the cotton-ramie (I_β-dominant) type. The differences between the two types of cellulose were clearly observed in the d -spacings of peak 1 (d_1) and peak 2 (d_2). The algal-bacterial type had larger d_1 and smaller d_2 values than the cotton-ramie type. The d_3 values depended not only on the I_α or I_β proportion, as shown in Fig. 1, but also on the FWHM, which varies inversely with the crystallite size. The d_3 values increased with increasing H_3 value.

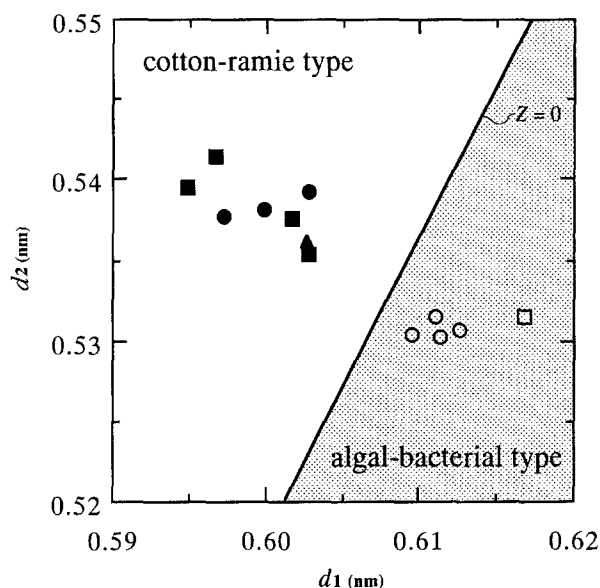
Discriminant analysis using d -spacing data from X-ray diffractometry^{8,14,20} is an easy and objective method for classifying all native celluloses as the I_α-rich type or the I_β-dominant type. In this study we tried to develop a simple method using discriminant analysis, in which only two parameters, d_1 and d_2 , were used. As a result, the analysis that discriminated the algal-bacterial type or the cotton-ramie type gave the function

$$Z = 1693d_1 - 902d_2 - 549 \quad (4)$$

Table 1. d -Spacings and FWHM of native celluloses derived from X-ray diffractometry

Cellulose sample	d -Spacings (nm)			FWHM (degree)		
	d_1	d_2	d_3	H_1	H_2	H_3
Algal-bacterial type						
<i>Valonia</i>	0.611	0.531	0.391	0.748	0.568	0.659
<i>Dictyosphaeria</i>	0.610	0.530	0.391	0.738	0.546	0.597
<i>Cladophora</i>	0.611	0.530	0.392	0.655	0.520	0.529
<i>Chaetomorpha</i>	0.610	0.530	0.391	0.778	0.574	0.644
Bacterial cellulose	0.617	0.532	0.394	1.424	0.949	1.371
Cotton-ramie type						
<i>Halocynthia</i>	0.603	0.536	0.390	0.915	0.684	0.773
Cotton	0.603	0.539	0.394	1.662	1.231	1.407
Ramie	0.600	0.538	0.394	1.898	1.454	1.722
Kouzo	0.597	0.538	0.395	1.970	1.367	1.831
Akamatsu	0.602	0.538	0.397	2.379	1.759	2.223
Douglas fir	0.603	0.535	0.399	2.693	1.771	2.418
Yachidamo	0.597	0.541	0.397	2.129	1.487	2.062
Red meranti	0.595	0.540	0.397	2.303	1.455	2.179

FWHM, full width at half-maximum

**Fig. 2.** Z plot of native celluloses. One can easily classify all native celluloses into the algal-bacterial type and the cotton-ramie type using this plot. Open circles, algae; open squares, bacterial cellulose; triangles, *Halocynthia*; filled circles, cotton, ramie, and kouzo; filled squares, wood

where $Z > 0$ for the algal-bacterial (I_α -rich) type and $Z < 0$ for the cotton-ramie (I_β -dominant) type. By substituting the d_1 and d_2 values listed in Table 1 into the above function, all native cellulose samples were classified into two groups without error, as shown in Fig. 2. Measuring the d_1 and d_2 values and plotting them on Fig. 2, one can easily classify all native celluloses into two types: the algal-bacterial type and the cotton-ramie type.

The ^{13}C NMR method has been widely used to investigate the two crystalline phases (I_α/I_β) of native celluloses. According to the results of ^{13}C NMR,^{16,17} low crystalline wood cellulose is the I_β -dominant type, but it includes substantial amounts of I_α phase compared to cotton and

Halocynthia celluloses. Newman,¹⁸ based on the ^{13}C NMR spectra, reported that softwood celluloses are associated with the I_α -rich type, whereas hardwood celluloses are associated with the I_β -dominant type. However, the evidence indicating the existence of a triclinic structure (I_α) in wood cellulose has not yet been confirmed by other methods, such as X-ray and electron diffraction.^{8,12,14,15} The d -spacings of wood celluloses derived from X-ray diffractometry profiles were for d_1 0.595–0.603 nm and for d_2 0.535–0.541 nm. These values are significantly different from the d -spacings of I_α -rich type celluloses (d_1 0.610–0.617 nm, d_2 0.530–0.532 nm). This result supports the previous result from diffraction methods that wood cellulose is dominant in monoclinic structure (I_β). Although it is not entirely clear thus far why results obtained from the ^{13}C NMR and diffraction methods are different, it may be due to the effects of noncrystalline substances such as lignin and hemicelluloses in addition to the lower crystallinity of celluloses.

Estimation of the I_α/I_β ratio in hydrothermally treated celluloses

It is known that hydrothermal treatment transforms I_α to I_β without loss of crystalline perfection. To obtain cellulose samples that have various I_α/I_β ratios, we carried out hydrothermal treatment on highly crystalline *Cladophora* cellulose at temperatures of 200° to 280°C for 30 min. Some X-ray diffractometry profiles of these hydrothermally treated samples are shown in Fig. 3. Three crystalline peaks shifted in characteristic directions with increasing treatment temperatures. The profile of the sample treated at 200°C was almost the same as the initial one; I_α did not transform to I_β by this treatment at 200°C. When the treatment temperature was increased to 240°C, peak 1 shifted in a wider-angle direction, and peaks 2 and 3 shifted slightly in lower- and wider-angle directions, respectively. The movement of these three peaks was also observed at 280°C. Although the peaks became somewhat broader owing to a decrease in

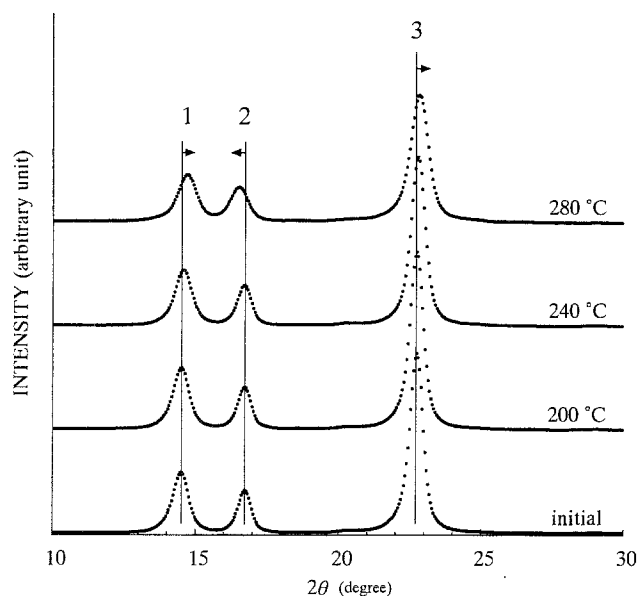


Fig. 3. X-ray diffractometry profiles of hydrothermally treated *Cladophora* cellulose

crystallite size or loss of crystalline perfection, the sample treated at 280°C still had high crystallinity. Therefore, the shift of these peaks was ascribable to the transformation from the I_α phase to the I_β phase.

By separating these three peaks, we determined the d -spacings (d_1 , d_2 , d_3) shown in Fig. 4. The d -spacings of the sample were not changed by treatment at temperatures of 200°–230°C; these values were almost the same as the initial ones. At treatment temperatures of 240°–250°C, d_1 and d_2 rapidly decreased and increased, respectively. In contrast, d_3 slightly decreased in the same temperature range. The d -spacings of the sample treated at 260°C became almost the same as those of I_β -type *Halocynthia* cellulose (Table 1). Above 260°C, every d -spacing was nearly constant. These changes in d -spacing indicated that the transformation from I_α to I_β may occur above the crystalline phase transition temperature at about 240°–250°C.

As the d -spacings d_1 and d_2 changed greatly during the transformation from I_α to I_β , we tried to estimate the I_α/I_β ratio of the sample by plotting them in Fig. 2. The d -spacings d_1 and d_2 are complexes of two d -spacings from two phases: d_1 is $d_{I_\alpha(100)}$ and $d_{I_\beta(1\bar{1}0)}$; and d_2 is $d_{I_\beta(110)}$ and $d_{I_\alpha(010)}$. These individual four d -spacings of *Cladophora* cellulose have been previously determined from synchrotron-radiation X-ray diffractometry profiles.¹² They are $d_{I_\alpha(100)} = 0.613$ nm; $d_{I_\beta(1\bar{1}0)} = 0.602$ nm; $d_{I_\beta(110)} = 0.535$ nm; and $d_{I_\alpha(010)} = 0.529$ nm. If the I_α/I_β ratio of a sample was 10:0 (pure I_α), d_1 0.613 nm and d_2 0.529 nm would result. On the other hand, if the I_α/I_β ratio is 0:10 (pure I_β), d_1 0.602 nm and d_2 0.535 nm would result. When the I_α/I_β ratio is x/y (where $x + y = 10$), d -spacings d_1 and d_2 can be represented as follows.

$$d_{1x/y}(\text{nm}) = 0.613 \frac{x}{10} + 0.602 \frac{y}{10} \quad (5)$$

$$d_{2x/y}(\text{nm}) = 0.535 \frac{y}{10} + 0.529 \frac{x}{10} \quad (6)$$

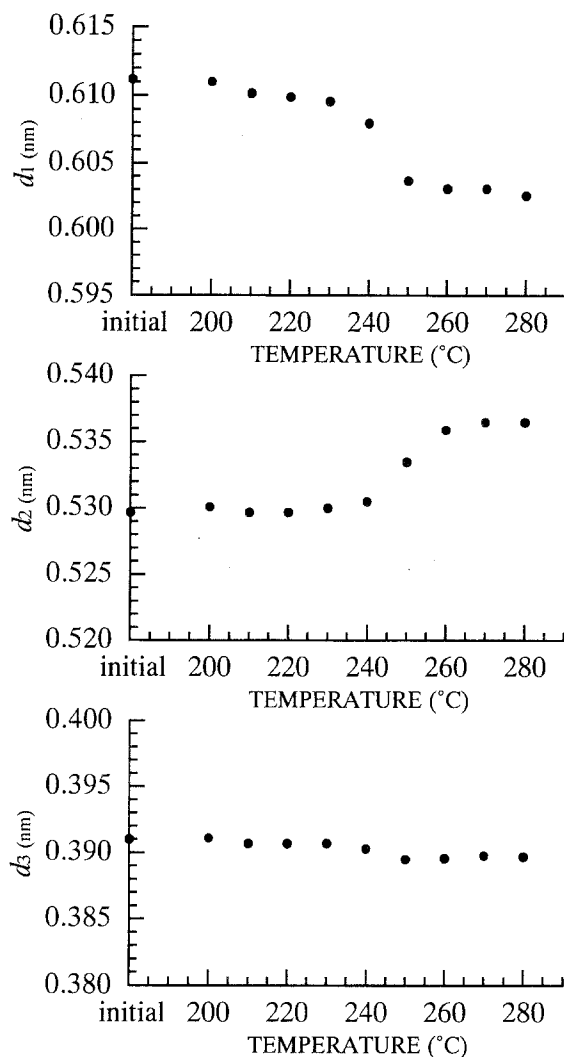


Fig. 4. Change in d -spacing with increasing hydrothermal treatment temperature

Considering the statistical error in the measurement, all points of d_1 and d_2 denote a line containing the point ($d_{1x/y}$, $d_{2x/y}$), which is parallel to the equation $Z = 0$ (see Eq. 4). The line that represents the relation between d_1 and d_2 in the case of various I_α/I_β ratios from 10:0 to 0:10 with 10 steps is shown in Fig. 5. The d_1 and d_2 values for hydrothermally treated samples of *Cladophora* are also plotted. The results indicate that the I_α/I_β ratio of the sample treated at 200° and 220°C, which was nearly equal to that of the initial *Cladophora*, varied from 8:2 to 7:3. When the samples were treated at 240° and 250°C, the I_α/I_β ratios were 6:4 and 2:8, respectively. Furthermore, the I_α/I_β ratio became almost 0:10, which means pure I_β , by treatment at 260° and 280°C. As described above, we could easily estimate the I_α/I_β ratio of the sample by measuring d_1 and d_2 and plotting them on Fig. 5. However, if the sample has an extraordinary uniplanar orientation or is of low crystallinity, the above method may not apply for estimation of the I_α/I_β ratio. For highly crystalline cellulose, which does not have a uniplanar orientation, this method is useful for estimating the I_α/I_β (triclinic/monoclinic) ratio.

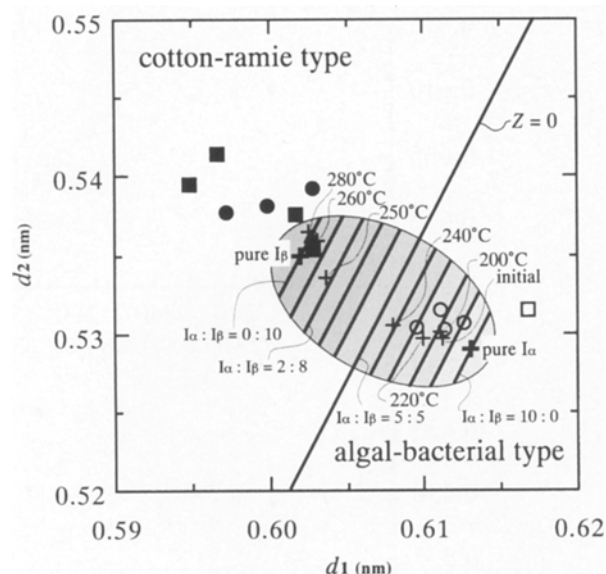


Fig. 5. Z plot of hydrothermally treated *Cladophora* cellulose. Each short straight line in the elliptic region represents the I_{α}/I_{β} ratio; +, hydrothermally treated *Cladophora* cellulose. Other cellulose species are also plotted (see Fig. 2 for explanation of the symbols)

Acknowledgments Part of this research was supported by Grants-in-Aid for Scientific Research (07406018 and 10760105) from the Ministry of Education, Science, Sports and Culture of Japan.

References

- Atalla RH, VanderHart DL (1984) Native cellulose: a composite of two distinct crystalline forms. *Science* 223:283–285
- VanderHart DL, Atalla RH (1984) Studies of microstructure in native celluloses using solid-state ^{13}C NMR. *Macromolecules* 17:1465–1472
- Horii F, Hirai A, Kitamaru R (1987) CP/MAS ^{13}C NMR spectra of the crystalline components of native celluloses. *Macromolecules* 20:2117–2120
- Sugiyama J, Vuong R, Chanzy H (1991) Electron diffraction study of the two crystalline phases occurring in native celluloses from an algal cell wall. *Macromolecules* 24:4168–4175
- Horii F, Yamamoto H, Kitamaru R, Tanahashi M, Higuchi T (1987) Transformation of native cellulose crystals induced by saturated steam at high temperatures. *Macromolecules* 20:2946–2949
- Yamamoto H, Horii F, Odani H (1989) Structural changes of native cellulose crystals induced by annealing in aqueous alkaline and acidic solutions at high temperatures. *Macromolecules* 22:4130–4132
- Sugiyama J, Okano T, Yamamoto H, Horii F (1990) Transformation of *Valonia* cellulose crystals by an alkaline hydrothermal treatment. *Macromolecules* 23:3196–3198
- Wada M, Sugiyama J, Okano T (1995) Two crystalline phase (I_{α}/I_{β}) system of native celluloses in relation to plant phylogeny. *Mokuzai Gakkaishi* 41:186–192
- Koyama M, Sugiyama J, Itoh T (1997) Systematic survey on crystalline features of algal celluloses. *Cellulose* 4:147–160
- Yamamoto H, Horii F (1993) CP/MAS ^{13}C NMR analysis of the crystal transformation induced for *Valonia* cellulose by annealing at high temperatures. *Macromolecules* 26:1313–1317
- Yamamoto H, Horii F, Hirai A (1996) In situ crystallization of bacterial cellulose. II. Influences of different polymeric additives on the formation of cellulose I_{α} and I_{β} at the early stage of incubation. *Cellulose* 3:229–242
- Wada M, Okano T, Sugiyama J (1997) Synchrotron-radiated X-ray and neutron diffraction study of native cellulose. *Cellulose* 4:221–232
- Kataoka Y, Kondo T (1999) Quantitative analysis for the cellulose I_{α} crystalline phase in developing wood cell walls. *Int J Biol Macromol* 24:37–41
- Wada M, Sugiyama J, Okano T (1994) The monoclinic phase is dominant in wood cellulose. *Mokuzai Gakkaishi* 40:50–56
- Wada M, Okano T, Sugiyama J, Horii F (1995) Characterization of tension and normally lignified wood cellulose in *Populus maximowiczii*. *Cellulose* 2:223–233
- Tanahashi M, Goto T, Horii F, Hirai A, Higuchi T (1989) Characterization of steam-exploded wood. III. Transformation of cellulose crystals and changes of crystallinity. *Mokuzai Gakkaishi* 35:654–662
- Lenholm H, Larsson T, Iversen T (1994) Determination of cellulose I_{α} and I_{β} in lignocellulosic materials. *Carbohydr Res* 261:119–131
- Newman RH (1994) Crystalline forms of cellulose in softwoods and hardwoods. *J Wood Chem Technol* 14:451–466
- Kataoka Y, Kondo T (1996) Changing cellulose crystalline structure in forming wood cell walls. *Macromolecules* 29:6356–6358
- Wada M, Sugiyama J, Okano T (1993) Native celluloses on the basis of two crystalline phase (I_{α}/I_{β}) system. *J Appl Polym Sci* 49:1491–1496
- Sugiyama J, Persson J, Chanzy H (1991) Combined infrared and electron diffraction study of the polymorphism of native celluloses. *Macromolecules* 24:2461–2466
- Nagaoka T, Oyanagi Y (1980) Program system SALS for nonlinear least-square fitting in experimental sciences. In: Matusita K (ed) Recent developments in statistical inference and data analysis. North Holland, Amsterdam, pp 221–225